Mon. Not. R. astr. Soc. (1979) **186**, 837–852

Circumstellar envelopes and the evolution of carbon stars

Martin Cohen *Department of Astronomy, University of California, Berkeley, California 94720, USA*

Received 1978 August 31; in original form 1978 April 21

Summary. A quantitative classification scheme is presented for carbon stars that yields temperature class, carbon class and C^{13} isotopic index, derived from low-resolution, image-tube scanner spectra. An absolute magnitude and bolometric luminosity calibration is constructed on the basis of temperature class from information existing in the literature. This scheme is applied to 16 carbon stars that have high infrared luminosity and results in spectral classifications; quantitative estimates of circumstellar extinction, both differential and neutral, assuming that small graphite grains are responsible; individual distances; column masses of graphite; intrinsic fluxes of Hα emission; a possible evolutionary sequence. The hypothesis that hydrogen emission is caused by shock waves is vindicated.

1 Introduction

Infrared astronomy has revealed a number of interesting facets of the evolution of carbon stars, in particular the existence of extensive, optically thick envelopes. The object IRC + 10216 is a fine example of this phenomenon. Its envelope is even visible optically as an extended elliptical patch. Several molecules have been recognized by their rotational transitions at microwave frequencies in a cloud surrounding this optical core. Unbiased 10-μm sky surveys (AFGL: Price & Walker 1976) include an appreciable number of hitherto unknown, optically faint carbon stars. Indeed, the fraction of carbon stars among these new sources exceeds that found for the earlier 2-μm sky survey (Neugebauer & Leighton 1969) and is comparable with that attributable to M giants among the AFGL objects (Cohen & Kuhi 1977). The abundance of late-type stars in infrared surveys reflects their history of extensive mass loss into circumstellar reservoirs, followed by condensation to particulates. The faintness of the optical counterparts may herald their ultimate optical disappearance as the accumulation of dust grains proceeds. It is presumed that the AFGL carbon stars represent the latest phases of evolution that we have observed for this type of star. In this paper an attempt will be made to quantify the extinction in these circumstellar shells and to put these stars into an evolutionary sequence. Conceptually, the scheme resembles that applied by Cohen & Kuhi (1976, 1977) to M giant-infrared sources which resulted in the optical demonstration of the existence of circumstellar envelopes and yielded at least approximate estimates of shell extinction. The scheme outlined below for the carbon stars is somewhat more involved due to the especial features of these objects.

2 The classification of faint carbon stars

The thrust of this paper is to derive quantitative information from optical spectra of carbon stars. It is easy to classify new infrared sources as carbon stars either on the basis of their 3.1-μm HCN/C_2H_2 absorption (Ridgway *et al.* 1976) or of their 10- to 13-μm SiC emission (Treffers & Cohen 1974). However, infrared spectroscopy is not yet sophisticated enough to determine the temperature and carbon classes for two-dimensional classification. Thus we must appeal to optical spectra noting, however, that many optical counterparts of AFGL objects are extremely faint ($V \gtrsim 16$).

All the optical spectra described herein were obtained on the Lick Observatory 3-m telescope, using the Cassegrain image-tube scanner (Miller, Robinson & Wampler 1976). Effective resolution is ~7 Å and the two regions of relevance here are λλ 4270–6710 and λλ 6300–8700. The most powerful, quantitative classification scheme for carbon stars is Yamashita's (1965, 1972) photographic scheme. I have, therefore, observed 34 carbon stars classified by Yamashita, with the same instrumental configuration (most on the 3-m telescope but some on a 0.7-m telescope equipped with an identical image-tube scanner). From this material, classification criteria can be established for the absolute flux, low dispersion scanner spectra. Table 1 presents the 'standard carbon stars' observed to establish the scanner scheme.

Table 1. Standard carbon stars observed and Yamashita types.

Star	Type	Star	Type	Star	Type	Star	Type
HD 5223	C1,2	HD 52432	C4,5	V460 Cyg	C6,3	V Cyg	C7,4
HD 182040	C2,2	VX And	C4,5	UX Dra	C6,3	TT Tau	C7,4
HD 16115	C2,3	NQ Cas	C4,5	VY Uma	C6,3	GP Ori†	C8,0
HD 223392	C3,2	AX Cyg	C4,5	RV Cyg	C6,4	RR Her	C8,1
VY And	C3,4	ST And	C5,3	RY Cyg	C6,4	RS Cyg	C8,2
TT CVn	C3,5	AQ And	C5,4	T Lyr	C6,5	WZ Cas	C9,2
V Ari	C4,4	TT Cyg	C5,4	Z Psc	C7,2	U Cyg*	C9,2
RV Mon	C4,4	WW Cas	C5,5	TX Psc	C7,2		
HD 19557	C4,5	Y CVn	C5,5	V Oph	C7,3		

* observed near minimum light
† SC

2.1 TEMPERATURE INDEX

The Na I D lines provide an excellent indicator of temperature at low dispersion (Yamashita 1972). I selected two points at λλ 5720, 6070 to interpolate the local 'continuum' at λ 5893 symmetrically placed with respect to the D lines to avoid difficulties with heavily reddened stars. These coincide with Yamashita's (1965) more precisely located continuum points at λλ 5716, 6073. The temperature index is then defined to be

$$T = 2I(5893)/[I(5720) + I(6070)].$$

Intensities from the scanner spectra are essentially monochromatic, spanning one resolution element (7 Å). Spectra were taken with large apertures, 8 arcsec square, to maintain photometric accuracy and most were obtained in good seeing (i.e. without degradation of spectral resolution) of $\lesssim 2$ arcsec. Table 2 indicates the mapping of Yamashita temperature class

Table 2. The relation between Yamashita temperature class and scanner index *T*.

Temperature class	Index T	No. of stars
1	0.86	1
2	0.68 ± 0.01	2
3	0.64 ± 0.02	3
4	0.50 ± 0.02	7
5	0.48 ± 0.03	4
6	0.44 ± 0.02	4
7	0.33 ± 0.02	4
8	0.26 ± 0.09	3
9	0.07 ± 0.03	2

against index *T*, together with rms errors of the mean in *T* and the number of stars used to define this mean.

2.2 CARBON INDEX

The Swan bands of C_2 are the obvious indicators of carbon abundance. I use the λλ 5165, 5635, 6192 bandheads and define one-sided indices

$$C1 = I(5165)/I(5185),$$

$$C2 = I(5635)/I(5660),$$

$$C3 = I(6192)/I(6195).$$

Table 3 shows the relation between Yamashita carbon class and these three indices in the manner of Table 2.

Table 3. The relation between Yamashita carbon class and scanner indices C1, C2, C3.

Carbon class	C1	C2	C3	No. of stars
0	0.79	0.79	0.88	1
1	-	0.73	0.96	1
2	0.49 ± 0.04	0.62 ± 0.04	0.87 ± 0.01	7
3	0.25 ± 0.03	0.40 ± 0.04	0.81 ± 0.04	6
4	0.20 ± 0.02	0.32 ± 0.02	0.65 ± 0.02	9
5	0.18 ± 0.02	0.29 ± 0.02	0.66 ± 0.03	9

2.3 NARROWBAND COLOUR INDICES

Cohen & Kuhi (1976, 1977) used narrowband scanner indices between λλ 5400, 6000 and 6700 to evaluate the total extinction for M giants among the AFGL sources. An analogous set of indices is required for carbon stars. I selected wavelengths λλ 5220, 5720 and 6615 after consideration of Yamashita's (1965) listed continuum points and of the appearance of typical carbon star spectra. An additional index that is useful is one between λ 6880 and λ 7830. Shortward of ~ 5000 Å it is extremely difficult to detect the AFGL carbon stars, so red are their continua. Longward of ~ 8500 Å there will almost certainly be contamination of photospheric flux due to overlying thermal emission by circumstellar dust grains. Table 4 defines the normal colours of carbon stars based on image-tube spectra of 32 stars in Table 1. It should be noted that the colours cited in Table 4 form a one-dimensional system and

Table 4. Narrowband colour indices for normal carbon stars.

Temperature class	[52,66]	[57,66]	No. of stars
1	0.49	0.19	1
2	0.43 ± 0.12	0.18 ± 0.03	2
3	0.95 ± 0.26	0.40 ± 0.08	3
4	1.34 ± 0.23	0.53 ± 0.08	7
5	1.70 ± 0.19	0.68 ± 0.04	5
6	1.81 ± 0.18	0.73 ± 0.03	5
7	1.82 ± 0.05	0.87 ± 0.04	4
8	1.95	0.88	1
9	1.97	1.00	1

depend only on temperature; no dependence upon carbon abundance was found for stars o the same temperature class. We define

$$[\lambda_1, \lambda_2] = 2.5 \log_{10} [I(\lambda_2)/I(\lambda_1)]$$

as the index between wavelengths λ_1 and λ_2, and adopt the shorthand [52, 66] and [57 66] for the two indices of relevance. It was necessary to exclude three stars from this norma colour grid of carbon stars, namely U Cyg, V Cyg and GP Ori. Their colours are much redde than other stars of the same temperature class.

Fay & Honeycutt (1972) have demonstrated that blackbody curves for roughly appro priate temperatures match the continua of carbon stars in some wavelength regions. Amon these are ~6900, ~7800 Å. The positions of apparently similar continuum peaks in m scanner spectra of carbon stars are λλ 6880, 7830. Therefore, it may be valuable to compar the ratio of continua at these two wavelengths with the ratio expected from a blackbody o appropriate temperature. The temperature scale for classes 2–9 is given in Table 5, adopte from Yamashita (1965, his figure 12).

Table 5. Temperature, absolute magnitudes, bolometric luminosity and stellar radius.

	C2	3	4	5	6	7	8	8–9	9
T^* (K)	3240	3050	2900	2760	2620	2510	2370	2300	2230
M_V	-1.9	-2.1	-2.3	-2.5	-2.6	-2.8	-2.9	-3.0	-3.1
M_R	-2.6	-2.8	-4.3	-4.4	-4.4	-4.7	-5.0	-5.1	-5.2
L_{bol} ($L_\odot$)	700	1700	3200	5500	9500	15100	28800	38000	50100
R^* (10^{13} cm)	0.6	1.0	1.6	2.3	3.3	4.6	7.1	8.6	10.5

2.4 C^{13} ISOTOPE

The isotopic shifts of molecular bandheads are readily seen in the spectra of carbon stars, i particular those due to C^{13} sequences as opposed to C^{12}. Bouigue (1954) and Gordon (1967 have commented upon the enhancement of the features at λ 6260 and λ 6168 in som spectra. Yamashita (1972) supplies an index of the strength of these bands. For low dispersion scanner spectra I define

$$CC = I(6168)/I(6191)$$

and

$$CN = I(6260)/I(6206),$$

as the ratios of flux at the $C^{12}C^{13}$ and $C^{12}C^{12}$ bandheads (λ 6168), and at the $C^{13}N$ and $C^{12}N$ bandheads (λ 6260). A survey of Yamashita's C^{13} indices show that there are effectively only four values, namely 3, 4, 5 and 0. Table 6 gives my mean scanner values corresponding to non-zero Yamashita index (stars of index zero do not have well-defined scanner indices as a group). I have assumed that the 24 standard stars used to define these indices do not suffer appreciable extinction, although the closeness in wavelength of the pairs of bandheads renders this a negligible or weak effect for normal stars.

The derivation of actual abundance ratios, as opposed to indices of C^{13}/C^{12}, is problematic especially at low spectral resolution. Ideally lines from individual rotational levels should be analysed. Curve of growth methods suffer from the extreme difficulty of estimating the true continuum levels in carbon stars. Model atmospheres provide more reliable abundance ratios but a satisfactory, generally accepted, grid does not yet exist for the atmospheres of carbon stars.

Table 6. C^{13} isotope indices.

Yamashita C^{13} index	CC	CN	No. of stars
3	1.14 ± 0.01	1.28 ± 0.02	14
4	1.02 ± 0.03	1.08 ± 0.04	6
5	0.95 ± 0.04	0.87 ± 0.02	4

3 Extinction – a theoretical scheme

For the M giants the narrowband colour excesses were converted into total extinctions by use of the usual law of interstellar extinction (Cohen & Kuhi 1977). This method is justified since these oxygen-rich stars (deduced from the presence of TiO and absence of ZrO bandheads) are thought to produce silicate grains, and since optical extinction in the interstellar medium is believed to be due predominantly to silicate grains. However, carbon star envelopes will be deficient in silicates, and abundant in graphite and SiC grains. Therefore, use of the normal interstellar law is suspect.

In general, carbon stars suffer both interstellar and circumstellar extinction and it is desirable to solve independently for both components. Consider the following routine. If A_C and A_I represent circumstellar and interstellar visual extinctions, respectively, then at any wavelength λ_i

$$I_i(\text{observed}) = I_i(\text{intrinsic})\, 10^{-0.4(\alpha_i A_C + \beta_i A_I)},$$

where $A(\lambda_i)/A(V) = \alpha_i$(circumstellar) or β_i(interstellar). For three such wavelengths, we find after manipulation

$$[\lambda_1, \lambda_3]_{\text{observed}} = [\lambda_1, \lambda_3]_{\text{intrinsic}} + (\alpha_1 - \alpha_3)\, A_C + (\beta_1 - \beta_3)\, A_I,$$

$$[\lambda_2, \lambda_3]_{\text{observed}} = [\lambda_2, \lambda_3]_{\text{intrinsic}} + (\alpha_2 - \alpha_3)\, A_C + (\beta_2 - \beta_3)\, A_I,$$

with the definition of colour indices $[\lambda_1, \lambda_2]$ above. In principle there is sufficient information to solve for A_C and A_I, provided that we understand the law of circumstellar extinction represented by the set of $\alpha_1\alpha_2\alpha_3$. Strictly, in a circumstellar environment we are not concerned with extinction but rather with absorption since scattered radiation is not lost, unlike the interstellar situation. The coefficients $\alpha_1\alpha_2\alpha_3$ are determined from the absorption efficiency factors for the grains (since $A(\lambda)/A(V) = \tau(\lambda)/\tau(V) = Q_{\text{abs}}(\lambda)/Q_{\text{abs}}(V)$). If $A_C \gg A_I$ we may take $A_I = 0$ and solve for A_C. This would represent an optically very thick shell around a relatively nearby carbon star, a probable situation.

In practice this scheme must be simplified. The simplest case arises for a shell consisting solely of graphite grains, spherical and of one size. The coefficients α_i are then obtainable from Mie scattering computations. The formal solution for $(\lambda_1\lambda_2\lambda_3) = (5220, 5720, 6615\,\text{Å})$, using a Whitford-type interstellar curve with $R = 3.10$ (Barlow & Cohen 1977), is

$$A_C = (1.7048[57, 66]_{XS} - [52, 66]_{XS})/E_C,$$

$$A_I = ([52, 66]_{XS} - E_I A_C)/0.2859,$$

where

$$E_C = 1.7048[(Q_{57} - Q_{66})/Q_V] - E_I,$$

$$E_I = (Q_{52} - Q_{66})/Q_V,$$

and Q signifies an absorption efficiency factor.

4 Absolute calibration

Gordon (1968) has reviewed the absolute magnitudes of carbon stars, and has incorporated bolometric corrections determined by Mendoza & Johnson (1965). However, she chose to use equivalent blue spectral types to describe the temperatures of carbon stars. I have redetermined the calibrations for M_{bol} and M_V using least squares linear fits to the absolute magnitude–temperature planes based upon Yamashita's temperature scale. The stars used for these calibrations were drawn from Gordon's (1968) table IV. They span the range of temperature class from C6 to C9, and almost all the stars in Table 8 lie within this range. V CrB seems to be a much more luminous star than the others of class C6; consequently it was omitted from the least squares fitting. However, inclusion of V CrB would alter the calibration of M_V by less than 0.2 and that of M_{bol} by less than 0.5 between C6 and C9. Final adopted luminosities should be accurate to better than a factor of 3. The multicolour photometry of carbon stars by Mendoza & Johnson (1965) provides mean $(V–R)$ colours. These yield a calibration for M_R, with inherent errors of order $(A_V–A_R)$, or $\sim 0.2 A_V$. I chose the optically brightest stars for which interstellar and circumstellar reddening should be minimal. Table 5 summarizes the various parameters of this calibration, including an estimate of stellar radius, R^*, based upon the assumption that Yamashita's scale represents effective temperature. For completeness this table is extrapolated to C2 stars but the absolute magnitude and luminosity calibrations are probably less accurate for the hotter stars than for the cooler.

5 The AFGL stars

5.1 CLASSIFICATION

We shall discuss 16 carbon stars that are AFGL infrared sources. Four are drawn from Cohen & Kuhi (1976), 10 from Cohen & Kuhi (1977), and IRC + 10216 and + 30219 are obvious candidates for inclusion. Lick spectra of all 16 are available from 4270 to 6710 Å, and spectra of nine of these are also available between 6300 and 8700 Å. These spectra were measured at the wavelengths designated above to determine temperature, carbon class, C^1 index and narrowband colours. Table 7 presents the indices formed from these measurements. Stars are designated by their running numbers in the AFGL catalogue for convenience and prefixes are suppressed.

The classifications follow immediately and Table 8 summarizes these, together with the colour excesses $[52, 66]_{XS}$, $[57, 66]_{XS}$ for each star. Also appended are the parameters for U Cyg, V Cyg and GP Ori.

Table 7. AFGL stars: indices and colours.

AFGL	C1	C2	C3	T	CC'	CN'	[52,66]	[57,66]	IRC
799	-	0.45	0.58	0.28	1.11	1.06	5.44	2.25	
1381	-	.79:	.53	.09	1.00	1.36	-	3.13	+10216
1403	-	.67	.72	.53	1.09	1.21	3.15	1.83	+30219
2118	-	.38:	.63	.12	1.13	1.22	5.92	2.31	
2232	0.45:	.47	.82	.31	1.23	1.39	3.72	1.48	+20370
2368	.17	.33	.72	.48	1.21	1.41	3.21	1.41	-10502
2392	.44	.39	.67	.33	1.11	1.28	4.07	1.87	
2428	.27	.29	.68	.56	0.85	0.89	2.20	0.80	
2679	.41:	.47	.88	.17	1.22	1.30	3.90	1.97	
2686	-	-	.51	.15	1.22:	1.13	-	2.71	
2699	.84	.49	.75	.20	1.26	1.18	3.48	1.68	
2704	-	.33:	.77	.43	1.11	1.24	4.91	2.31	+50357
2881	-	.60	.82	.20	1.00	1.10	7.48	3.16	
2985	-	.43	.67	.21	1.17	1.27	6.06	2.34	
3011	-	-	.90:	.00	-	-	5.12	3.24	
3116	-	-	.75:	.20	1.08	1.15	5.77	3.70	+40540
U Cyg					1.27	1.60			
V Cyg					1.02	1.09			
GP Ori					1.08	1.20			

Table 8. AFGL stars: classification, colour excesses and C^{13} isotopic index.

AFGL	Classification	$[52,66]_{XS}$	$[57,66]_{XS}$	C^{13} index
799	C8,4	3.49	1.37	4
1381	C9,5	-	2.25	3:
1403	C4,3	1.81	1.30	3:
2118	C9,4	3.95	1.31	3
2232	C7,3	1.90	0.61	2:
2368	C5,4	1.51	0.73	2:
2392	C7,3	2.25	1.00	3
2428	C4,4	0.78	0.25	5
2679	C8-9,2	1.94	1.03	3
2686	C8-9,5	-	1.77	4:
2699	C8,3	1.53	0.80	2-3
2704	C6,4	3.10	1.58	3
2881	C8,3	5.53	2.28	4
2985	C8,4	4.11	1.46	3
3011	C9,2	3.15	2.24	-
3116	C8,3.5	3.82	2.82	4
U Cyg	C9,2	2.22	0.61	< 2
V Cyg	C7,4	2.79	0.81	4
GP Ori	C8,0	0.78	0.50	3-4

5.2 FORMAL SOLUTIONS FOR EXTINCTION

I have computed the values of the absorption efficiency factors at the relevant wavelengths for spherical graphite grains of radius 0.01, 0.025, 0.04, 0.06, 0.08 and 0.1 μm. To obtain physically meaningful solutions for A_C, A_I using the method described above (Section 3), requires a grain size such that E_C has the same sign as the numerator of A_C. For the above sequence of grain radii, E_C has the values 0.0005, -0.0052, -0.0113, 0.0031, 0.0483, 0.0215. Physical solutions exist for only four stars, requiring 0.08 μm grain radius in each case. These solutions do seem credible, in general, since the interstellar components of extinction are much smaller than the circumstellar. In all other cases an unphysical value of A_I results (negative) for all grain radii.

The formal method of solution does involve quite small denominators and it is valuable to investigate the sensitivity of the method to probable errors in the colour excesses. For example, if we attribute errors of ±0.05 to the excesses in CRL 1403, the resulting four combinations of colour excess yield values of A_C from 5.6 to 9.1, and of A_I from 1.1 to 3.2 together with one negative value. It is entirely possible that errors of ±0.05 exist in the determination of standard colours (*cf.* Table 4). Consequently, the four solutions in Table 9 should perhaps be regarded only as qualitatively indicative of the true situation.

A further complication arises in the implicit assumption that graphite particles alone contribute to the extinction between 5200 and 6600 Å. For example, SiC grains also produce an opacity at short (violet) wavelengths (Gilra & Code 1971) and it could be that in extreme cases this opacity is seen in the green region.

Table 9. Formal extinction solutions for four stars.

Star	A_C	A_I
1403	8.4	1.4
3011	13.9	2.9
3116	20.5	1.3
GP Ori	1.5	1.8

5.3 SIMPLER SOLUTIONS FOR EXTINCTION

Henceforth we shall assume that graphite opacity is predominant in the circumstellar shells. Further we shall adopt the simplification $A_I = 0$. There are three independent types of solution for A_C, from $[52, 66]_{XS}$, $[57, 66]_{XS}$ and from the ratio of fluxes at 6880 and 7830 Å. Each of these three methods yields a value of A_C dependent upon assumed grain radius (in the range 0.01–0.08 μm; grains of radius 0.1 μm actually produce differential 'blueing'). Table 10 presents the various values of A_C deduced for two representative stars. It should be noted that, just as another opacity source may contribute at 5200 Å, so thermal emission by dust grains may add flux at 7830 Å. (If the temperature of such grains were

Table 10. Values of A_C determined by three methods for two representative stars.

2704					
Radius (μm)	.01	.025	.04	.06	.08
Method					
$[52,66]_{XS}$	12.5	10.7	9.1	8.9	18.4
$[57,66]_{XS}$	10.8	9.5	8.2	7.7	12.4
$(6880,7830)_{XS}$	15.1	14.1	13.4	12.4	11.1

3116					
Radius (μm)	.01	.025	.04	.06	.08
Method					
$[52,66]_{XS}$	15.4	13.2	11.2	11.0	22.7
$[57,66]_{XS}$	19.3	16.9	14.6	13.7	22.2
$(6880,7830)_{XS}$	13.9	12.9	12.3	11.4	10.2

~1000 K then there would be appreciable extra flux at 7830 Å but relatively little at 6615 Å.) These two problems would manifest themselves, respectively, by making $A_C(52, 66) > A_C(57, 66)$, and $A_C(68, 78) > A_C(57, 66)$. Table 11 summarizes (in columns 2 and 3) the mean (with respect to grain size) values and ranges of A_C determined for the 19 stars in Table 7 from optical and/or near-infrared means. Generally, when extinctions have been determined from both optical and near-infrared data, these ranges overlap.

5.4 HYDROGEN EMISSION LINES

$H\alpha$ emission is not common among normal carbon stars. It occurs in the spectra of only six of the coolest stars in Table 1, a conclusion noted also by Gordon (1967). However, among the AFGL stars it is essentially the norm. Only 799 and 2428 do not show it. Emission at $H\beta$ is also seen for six AFGL stars and the ratio of intensities at $H\alpha$ and $H\beta$ yields another estimate of extinction for these objects. We shall assume that the emission arises from radiative recombination and that the intrinsic ratio of the lines is $\log I(H\alpha)/I(H\beta) = 0.45$ (Brocklehurst 1971). Knowledge of the absorption efficiency factors for graphite grains at 4861 and 6563 Å then yields the total visual extinction. Strictly these estimates are only upper limits since we do not also know the ratio of $H\beta$ to $H\gamma$. They are included in Table 11 (column 4) represented by the average and range in extinction over the grain sizes 0.01, 0.025, 0.04 and 0.06 μm (radius 0.08 μm yields a far higher extinction due to the coincidental similarity of Q_{abs} at the wavelengths of $H\alpha$ and $H\beta$). These values are generally in agreement with those determined by other means for individual stars. The fluxes observed in $H\alpha$ emission were computed for all possible stars, as were the equivalent widths of emission (Table 11, column 10).

5.5 SHELL COLUMN MASS

If we assume that graphite is the crucial source of opacity in the optical region then the extinction, A_C, can be converted directly into a column density of particles. I have chosen

Table 11. Extinction, distance and shell parameters for carbon stars.

Star	A_C (optical)	A_C (near-infrared)	A_C ($H\alpha/H\beta$)	$M(57,66)$ (10^{-4} g cm^{-2})	S	D (kpc)	A_V(DM)	A_N	EW($H\alpha$) (Å)	T_S (K)	R_S (10^{15} cm)
799	12.5 ± 3.5			1.4	12	4.31	5	7 ± 3.5	0	780	0.9
1381	14 ± 3	12 ± 2		2.3	14	0.22	18	5 ± 3	3.8	520	2.8
1403	8 ± 2	10.5 ± 1.5	6 ± 1	1.4	7	0.19	13	4.5 ± 2	11.3	650	0.5
2118	13 ± 4			1.4	13	2.94	6		4.6	990	0.8
2232	6 ± 2	5 ± 0.5	11.5 ± 2	0.6	10	0.79	6.5		14.3	840	0.6
2368	6 ± 2		8 ± 1.5	0.8	9	0.53	8		11.9	750	0.4
2392	8 ± 2			1.0	10	2.08	6		12.4	870	0.6
2428	2 ± 1			0.3	8	1.76	6.5	4.5 ± 1	0	760	0.3
2679	7.5 ± 2		16 ± 3	1.1	10½	4.56	5		20.6	870	0.9
2686	11 ± 2			1.8	13½	1.65	10		10.0	690	1.4
2699	6 ± 2	6.5 ± 1	7 ± 1.5	0.8	11	2.93	9		9.9	750	1.0
2704	12 ± 3	13 ± 2	13 ± 2	1.6	10	1.10	11		9.4	830	0.5
2881	22 ± 8	10 ± 1.5		2.4	11	3.11	7		0.3	850	0.8
2985	14 ± 4	6 ± 1		1.5	12	2.96	6		10.5	780	0.9
3011	14 ± 4	10 ± 1.5		2.3	11	4.21	11		2.7:	670	1.7
3116	18 ± 4	12 ± 2		2.9	11½	0.96	13		1.7:	650	1.4
U Cyg	7 ± 2			0.7	11	2.50	2		0.7:		
V Cyg	9 ± 2.5			0.9	11	0.61	6		3.0		
GP Ori	3.5 ± 1			0.5	8	2.06	2		2.4		
Column	(2)	(3)	(4)	(5)	(6)	(7)	(8)	(9)	(10)	(11)	(12)

to work solely with A_C determined from $[57, 66]_{XS}$ because of the potential contaminan at shorter and longer wavelengths. Thus

$$A_C = 1.086\,\tau(V) = 1.086\,N(a)\,Q_{abs}(a, V)\,\pi a^2,$$

for grain radius a, where $N(a)$ is the column density, and

$$M = 1.33\,\pi a^3 \rho N(a)$$

is the column mass in g cm^{-2}. Consequently

$$M = 2.46 \times 10^{-6} A_C(a)\,a/Q_{abs}(a, V),$$

where a is now in units of 0.01 μm. Column 5 of Table 11 gives the average value of M, con puted for each star from the individual colour excesses $[57, 66]_{XS}$ for the five grain rad 0.01–0.08 μm. These masses are based upon only differential extinction and cannot repr sent very large grains ($a \gtrsim 0.1\,\mu$m) that produce neutral extinction in the spectral region (interest. However, it may be reasonble to assume that the total amount of neutrally exti guishing material is proportional to the column mass in small grains. Under this assumptic M would represent the total shell mass.

5.6 DISTANCE

The temperature classification of stars in Table 8 indicates their bolometric luminosity (fro Table 5) and, if photometry exists to sufficiently long wavelengths ($\lambda \geq 3.5\,\mu$m), integratic under the broadband energy distributions yields distances. There are various sources in tl literature for these infrared data: 799, 2699, 2881 and 3011 (Gehrz & Hackwell 197 2118, 2392, 2428 and 2686 (Lebofsky *et al.* 1976); 2232, 2704 and 3116 (Strecker & N 1974a); 1381 and 1403 (Strecker & Ney 1974b); 2368 (Merrill & Stein 1976); 2985 (Pri & Walker 1976, no ground-based photometry published); 2118 and 2392 (short wavelengt photometry from Allen *et al.* 1977). Additional data were used for 2679, 2686 (Hudsc 1977, private communication), U Cyg (Cohen, unpublished; Gehrz & Woolf 1971), V C (Forrest, Merrill & Stein 1975), GP Ori (Merrill 1978, private communication).

The integrations were performed for $\lambda \geq 1.6\,\mu$m and extended to infinity (Cohen 197 No corrections for extinction were applied to the infrared data since this attenuation occu primarily in the circumstellar envelope, and no optical luminosity was included (except f U Cyg, V Cyg and GP Ori) since this energy is already represented by the infrared flu Distances are given in column 7 of Table 11.

5.7 NEUTRAL EXTINCTION

Distance moduli can be determined by two different methods: $5 \log D - 5$ and $V - A_V - M$ (or $R - A_R - M_R$). Comparison of the former with the latter yields an estimate of A_V or A ($\sim 0.80 A_V$ for graphite particles), designated as A_V(DM) in Table 11 (column 8). For mo stars, A_V(DM) lies within the various ranges cited for A_C. However, for four objects A_V(D significantly exceeds A_C and these excesses may be due to neutral circumstellar extinctic by large grains, A_N in Table 11 (column 9). Due to the sizeable range in A_C for any speci star it is generally difficult to recognize a value of A_N less than ~3 mag. Consequently, it quite possible that all objects suffer neutral extinction but to a lesser degree than these fo stars. This does suggest, however, that the column mass determined from differential extin tion may not be proportional to the total column mass through the shells, for all stars.

5.8 THE C^{13} ISOTOPE

Indices of C^{13} were measured for all stars. These have been corrected for extinction using differential extinction curves averaged over a range of radii for small graphite grains. Corrected indices appear in Table 7 (CC′, CN′) and deduced C^{13} indices (on the Yamashita system) are given in Table 8. The optical spectrum of 3011 is somewhat noisy around 6200 Å and no C^{13} index has been determined.

5.9 NEAR-INFRARED SPECTRA

The spectra of the various stars between 6300 and 8700 Å are remarkably similar to one another. All are dominated by CN systems ($\Delta v = 2, 3$); C_2 bandheads are also strong; isotopic features of $C^{13}N^{14}$ and $C^{12}C^{13}$ are readily recognizable; lines of Na I (λλ 8183, 8195) and K I (λ 7699) are in absorption, as are lines of the Ca II triplet in most stars. However, it has not been possible to obtain a spectral classification based upon these infrared characteristics and such a scheme would be suspect, since thermal emission by grains must begin to overlie these spectra, rendering bandhead and line strengths unreliable as indicators of temperature, atomic or molecular abundances.

5.10 CO CLOUDS

Microwave CO emission has been observed from several AFGL carbon stars: 1381 and 1403 (Wilson, Schwartz & Epstein 1973; Mufson & Liszt 1975), 2232 and 3116 (Zuckerman *et al.* 1977). Upper limits of ~0.2 K in antenna temperature (with the NRAO 11-m dish) have been obtained for 2368, 2392, 2428, 2686 (Zuckerman *et al.* 1977). It is interesting to note that the four stars detected in CO are among the closest of the AFGL stars to us (Table 11), and the two whose clouds are resolved (1381 and 1403) are the two closest (however, see the note concerning the distance to 1403 below).

5.11 THE CIRCUMSTELLAR ENVELOPES

The condensation into grains of outflowing gas in carbon stars would be expected to depend upon both photospheric temperature and carbon abundance. The cooler the star, the more readily could condensation occur; and the higher the carbon abundance, the greater the available number of condensation nuclei. There is no dependence of column mass M on either temperature or carbon class, separately. However, a very simple parameter that represents these two effects together is the sum of the temperature and carbon classes from the classification scheme. This parameter, S, is included in Table 11 (column 6). Fig. 1 tests this expected dependence in a plot of M against S. This is clearly an over-simplification of the condensation. In reality the velocity of outflow of gas also may affect the rate of condensation but this velocity is not readily estimated from observations.

The high frequency of occurrence of Hα emission among the AFGL stars suggests that this may be an important clue to the dynamics and evolution of the circumstellar shells. In Miras, the Balmer lines, particularly Hα, are deeply cut up by overlying TiO structure. However, in carbon stars, the same region does not suffer comparable mutilation. A study of a collection of high dispersion red spectrograms of carbon stars obtained by Wallerstein and Phillips shows that the rotational structure of CN is more 'open' than that of TiO, and Hα is quite visible through it without appreciable mutilation. Further, the absorption strengths of the CN features are less than those due to TiO in this spectral region. Therefore, some reliance may be placed upon the low resolution measures of total Balmer emission in

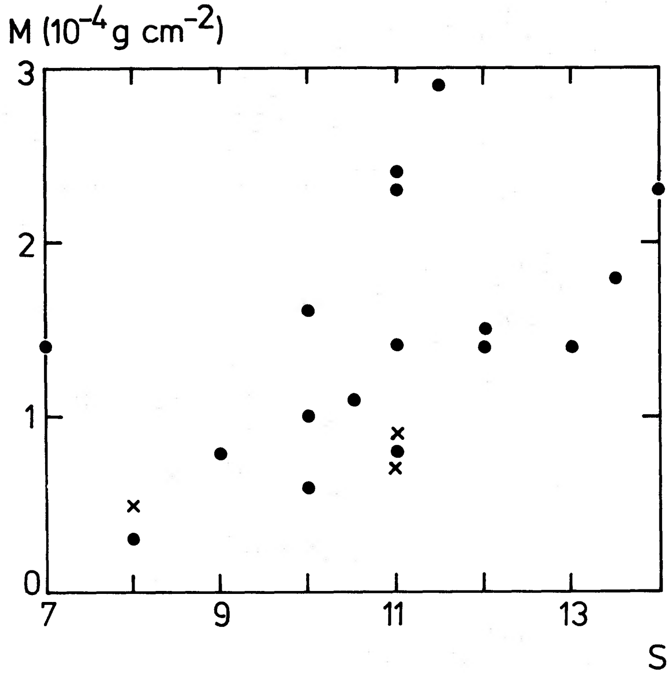

Figure 1. The dependence of shell thickness on temperature and carbon class: shell column mass M against S (sum of temperature and carbon classes). U Cyg, V Cyg and GP Ori are represented by crosses 1403 is the point on the left edge.

carbon stars. It is believed that, in long-period variables, Hα emission is a consequence of shock waves originating from somewhere below the photosphere and rising through the outer stellar layers. If the phenomenon in the AFGL stars is related to this we expect both Hα and the underlying continuum to suffer the same extinction. In support of this, Fig. 2 compares the flux of Hα, corrected for distance and neutral extinction but not for differential extinction, with M. The relationship shown in the plot strongly suggests that both Hα and the continuum suffer extinction by the same circumstellar material. The dust shells are thus much larger than both the photospheres and the more extended regions in which supersonic shocks collisionally excite the hydrogen gas.

This justifies a further correction to the Hα flux for the differential extinction of the continuum, A_C. A plot of absolute Hα flux against M shows no trend at all but does indicate that almost all the intrinsic Hα fluxes lie between 10^{34} and 10^{35} erg/s. Model atmospheres for late-type giants with hydrogen emission (Toy 1978, private communication) suggest that $N_H \sim 10^{13}\,cm^{-3}$ in the zone in which the emission arises. If we take a region in which $N_e = N_H$, appropriate to a shocked zone, we can test this shock wave picture for self consistency. An intrinsic Hα flux of a few $\times 10^{34}$ erg/s requires emission from a volume of a few $\times 10^{32}\,cm^3$ (using Case B recombination theory for $T_e = 10^4$ K). If the emission were to come from a thin spherical skin close to the photosphere then the thickness of this skin (for a typical cool photosphere of radius $\sim 7 \times 10^{13}$ cm) would be ~ 7000 cm, extremely shallow. Alternatively, expressed as a filling factor for the photospheric volume, the hydrogen emission arises in about 10^{-9} of this available volume. Therefore, the hypothesis of shock excitation of hydrogen emission seems vindicated.

The dust shells are characterized by cool blackbody curves beyond 2 or 3 μm. Shell temperatures, T_S, are incorporated into Table 11 (column 11). Estimates of shell radii, R_S can be made on a more secure footing than a simplistic black sphere calculation. Typically the stellar photospheres have $T^* \sim 2400$ K, with flux (F_λ) peaking at ~ 1.2 μm, while the

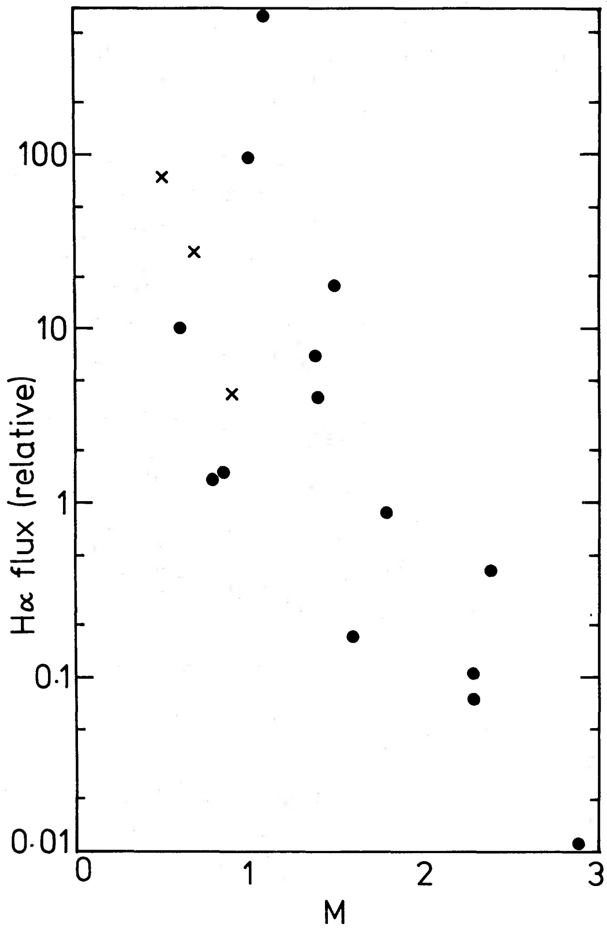

Figure 2. Relative fluxes of Hα emission, corrected for neutral extinction and distance, against shell column mass M. Symbols as in Fig. 1.

dust shells have $T_S \sim 750$ K and peak at $\sim 4.0\,\mu$m. Therefore, the equation of energy balance for grains, weighted by the peak fluxes of star and shell, gives, approximately

$$R_S = \frac{R^*}{2}\left(\frac{T^*}{T_S}\right)^2\left[\frac{Q_{abs}(1.2\,\mu m)}{Q_{abs}(4.0\,\mu m)}\right]^{1/2}.$$

R_S is given in Table 11 (column 12), The only direct check upon R_S is from 1381. Lunar occultation data (Toombs *et al.* 1972) indicate that this source has an inner core (of colour temperature ~ 600 K) of radius 0.22 arcsec and an outer, cooler (~ 375 K) shell of radius ~ 1 arcsec. Support for these values comes from 5-μm spatial interferometry of 1381 by McCarthy & Low (1975) who obtain 0.22 and 0.8 arcsec for the shells. The apparent radius of the dust cloud described in Table 11 would be 0.9 arcsec, in satisfactory agreement with the above number for the outer shell, although there can be no simple substitute for a solution to the radiative transfer problem.

Fig. 3 presents a plot of the equivalent width of Hα emission against column mass M. There are two rather different interpretations of the correlation. If Hα emission is a direct measure of the energy available to drive mass loss then we find that those stars with the highest (instantaneous) mass loss rates are the stars with the sparsest dust shells. The stars which have already accrued thick dusty envelopes have much smaller rates of mass loss. This argues that objects like 3116 are the most evolved carbon stars in the AFGL sample. Alterna-

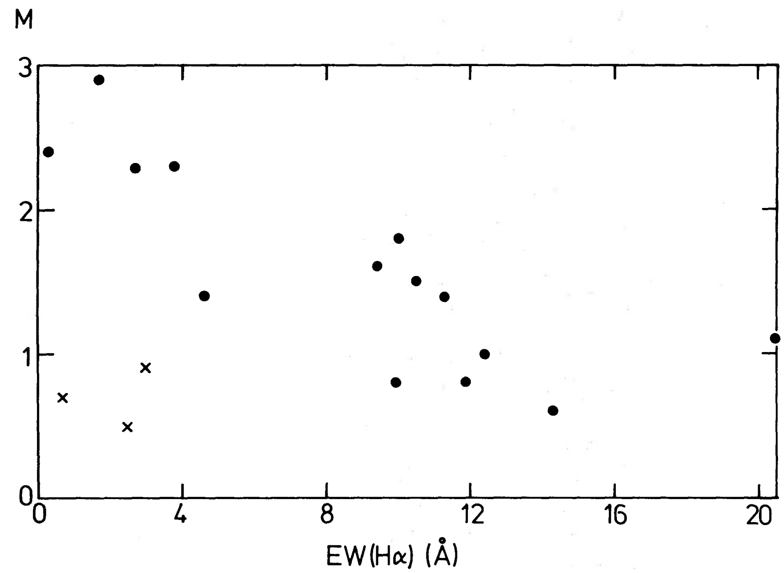

Figure 3. Shell column mass M against equivalent width of Hα emission. Symbols as in Fig. 1.

tively Fig. 3 may signify that there exist stars with large gas/dust ratios (like 2232) while others have far smaller ratios (like 3116). If this latter picture is relevant then no evolutionary interpretation arises, since neither temperature nor carbon class (nor S) accounts for the distribution of points in Fig. 3.

6 Retrospect

(1) On the basis of low-resolution image-tube spectra I have constructed a spectral classification scheme for carbon stars that yields temperature class (Na D lines), carbon class (C_2 Swan bands) and C^{13} index (λλ 6168, 6260 heads) in Yamashita's (1972) system. This scheme also provides standard 'continuum' colours between small, carefully selected spectral regions.

(2) I have optical and near-infrared spectra for a sample of 16 carbon stars from the AFGL infrared survey. Two-dimensional spectral classifications and C^{13} indices are given.

(3) The abnormally red colours of these stars have been converted into extinctions by assuming that small spherical grains of graphite are responsible. For four stars it is possible to obtain both interstellar and circumstellar components of extinction. However, extinctions for the whole sample have been obtained on the premise that $A_C \gg A_I$ and A_I was set to zero for these solutions. To avoid contamination of the colour excesses by thermal emission of dust grains (near-infrared) and by other possible opacity sources (green region), one standard colour excess $[57, 66]_{XS}$ was used. Column masses of small graphite grains were determined for the lines of sight through the dust shells.

(4) An absolute (M_V, M_R, L_{bol}) calibration for carbon stars has been constructed from the literature and this provides individual distance estimates for the AFGL stars.

7 Cautionary statements

The following cautionary statements are in order before we list the conclusions of this work.

(1) Small grains of materials other than graphite may be present and these would affect the values of A_C derived from colour excesses, hence the values of A_N.

(2) A distribution of grain sizes may be present in the circumstellar shells, rather than

single size distributions. However, if the size spectrum of circumstellar particles resembles that in the interstellar medium, the power law discussed by Mathis, Rumpl & Nordsieck (1977) may be of relevance. This law is quite steep and the optical properties of such a spectrum would closely approximate those of a single size distribution corresponding to the smallest particle size present.

(3) The spectra obtained for the AFGL stars are implicitly assumed to represent the stars at all times. Little is yet known about the variable nature of these stars, for example, if they are carbon Miras. The infrared energy distributions of some do vary (Price & Walker 1976). It is not known if the optical spectra also change. However, in the case of 1403 a little more information is available. The location of this star in Fig. 1 is suspicious. An old scanner spectrum of 1403 taken in 1974 shows no C_2 Swan bands, and even shallower Na D lines than the 1977 spectrum. The simplest explanation would be that the entire optical spectrum is overlaid by thermal emission of hot dust grains, masking the photospheric features. Consequently the type C4,3 may not accurately represent the photosphere which could be characterized by much deeper D lines (cooler) and more prominent C_2 bands (higher carbon class). The distance derived would thus be only a lower limit for this star. However, it is not likely that this is a general problem for the AFGL stars. One manifestation of this overlying emission is that A_C(near-infrared) > A_C(optical) and, as Table 11 shows, 1403 is the only star for which this holds true. Secondly the D lines would be a very sensitive indicator of excess continuum flux yet most AFGL stars reveal very deep D lines. Therefore, general veiling is improbable at λλ 5165, 5635 and the D lines, and the spectral classifications of most objects should not be appreciably distorted.

8 Conclusions

(1) The AFGL carbon stars have preferentially the coolest temperature classes, perhaps a tendency towards the highest carbon classes, and no preference as to C^{13} index.

(2) Typical circumstellar extinctions (attributed to small grains of graphite) are of order 5–15 mag. The corresponding column masses are of order $10^{-4}\,\mathrm{g\,cm^{-2}}$.

(3) Knowledge of the distance enables a test to be made for obvious neutral extinction, perhaps caused by very large grains. Typical values of neutral extinction that can be recognized easily are of order 5 mag.

(4) Hα emission occurs in all but two AFGL stars, supporting the conclusion that they are among the coolest of carbon stars. Stars with large equivalent widths of Hα have small values of column mass.

(5) For typical AFGL stars, photospheric radius (via L_{bol} and T^*) is 5×10^{13} cm, the zone in which Hα emission arises has a very small filling factor of the available photospheric volume, and the characteristic radius of the dust shell is 10^{15} cm. If 1381 is representative of the entire class there is an outer (cooler) dust shell of radius $\sim 2 \times 10^{15}$ cm and a CO molecular cloud of radius $\sim 10^{17}$ cm. Dust shells are characterized by colour temperatures of 500–1000 K. A crude estimate of the mass in the inner dust shell in small graphite grains is $3 \times 10^{-7} M_{\odot}$.

(6) The simplest, plausible evolutionary sequence for carbon stars might be one in terms of $\dot{M}$: larger $\dot{M}$ means greater degree of evolution. Such a scheme would naturally embrace the optically bright carbon stars too.

Acknowledgments

It is a pleasure to thank L. V. Kuhi for his collaboration in obtaining the image-tube spectra on the 3-m telescope and for a critical reading of the manuscript. I am indebted to

J. Stauffer for his contributions to the grid of standard carbon star spectra obtained during his time on the Lick 0.7-m telescope with its image-tube scanner. Many people contributed ideas and valuable discussion and I should like to thank in particular W. Fawley, J. Mathis, J. Phillips, H. Spinrad, L. Toy, G. Wallerstein and A. Zook. The Lick 3-m scanner was supported by the National Science Foundation under grant GP-29684. MC was supported by NSF grants AST 74-08151 and 75-13511.

References

Allen, D. A., Hyland, A. R., Longmore, A. J., Caswell, J. L., Goss, W. M. & Haynes, R. F., 1977. *Astrophys. J.*, **217**, 108.
Barlow, M. J. & Cohen, M., 1977. *Astrophys. J.*, **213**, 737.
Bouigue, R., 1954. *Ann. d'Astrophys.*, **17**, 104.
Brocklehurst, M., 1971. *Mon. Not. R astr. Soc.*, **153**, 471.
Cohen, M., 1973. *Mon. Not. R. astr. Soc.*, **164**, 395.
Cohen, M. & Kuhi, L. V., 1976. *Publs astr. Soc. Pacif.*, **88**, 535.
Cohen, M. & Kuhi, L. V., 1977. *Publs astr. Soc. Pacif.*, **89**, 829.
Fay, T. & Honeycutt, R. K., 1972. *Astr. J.*, **77**, 29.
Forrest, W. L., Merrill, K. M. & Stein, W. A., 1975. *Astrophys. J.*, **195**, 424.
Gehrz, R. D. & Hackwell, J. A., 1976. *Astrophys. J.*, **206**, L161.
Gehrz, R. D. & Woolf, N. J., 1971. *Astrophys. J.*, **165**, 285.
Gilra, D. P. & Code, A. D., 1971. *Bull. Am. astr. Soc.*, **3**, 279.
Gordon, C. P., 1967. *PhD dissertation*, University of Michigan.
Gordon, C. P., 1968. *Publs astr. Soc. Pacif.*, **80**, 597.
Lebofsky, M. J., Kleinmann, S. G., Rieke, G. H. & Low, F. J., 1976. *Astrophys. J.*, **206**, L157.
Mathis, J., Rumpl, W. & Nordsieck, K. H., 1977. *Astrophys. J.*, **217**, 425.
McCarthy, D. W. & Low, F. J., 1975. *Astrophys. J.*, **202**, L37.
Mendoza, E. E. & Johnson, H. L., 1965. *Astrophys. J.*, **141**, 161.
Merrill, K. M. & Stein, W. A., 1976. *Publs astr. Soc. Pacif.*, **88**, 294.
Miller, J. S., Robinson, L. B. & Wampler, E. J., 1976. *Advances in Electronics and Electron Physics*, Academic Press, New York.
Mufson, S. L. & Liszt, H. S., 1975. *Astrophys. J.*, **202**, 183.
Neugebauer, G. & Leighton, R. B., 1969. *Two micron sky survey: a preliminary catalogue*, NASA SP-3047.
Price, S. G. & Walker, R. G., 1976. *AFGL infrared sky survey*, Environmental Research Papers, No. 576.
Ridgway, S. T., Hall, D. N. B., Kleinmann, S. G., Weinberger, D. A. & Wojslaw, R. S., 1976. *Nature*, **264**, 345.
Strecker, D. W. & Ney, E. P., 1974a. *Astr. J.*, **79**, 797.
Strecker, D. W. & Ney, E. P., 1974b. *Astr. J.*, **79**, 1410.
Toombs, R. I., Becklin, E. E., Frogel, J. A., Law, S. K., Porter, F. C. & Westphal, J. A., 1972. *Astrophys. J.*, **173**, L71.
Treffers, R. R. & Cohen, M., 1974. *Astrophys. J.*, **188**, 545.
Wilson, W. J., Schwartz, P. R. & Epstein, E. E., 1973. *Astrophys. J.*, **183**, 871.
Yamashita, Y., 1965. *Publ. Dom. Astrophys. Obs.*, **XII**, 293.
Yamashita, Y., 1972. *Ann. Tokyo astr. Obs.*, **13**, 169.
Zuckerman, B., Palmer, P., Morris, M., Turner, B. E., Gilra, D. P., Bowers, P. F. & Gilmore, W., 1977. *Astrophys. J.*, **211**, L97.